Coexistence Nexus in practice: integrating One Health into the food-biodiversity challenge in Central America.

Voinson M.[1†], Crespin S.J.[2,3*], Escobar D.[4*] Moreno M. [5*], Castillo L.[5], Coto Hernandez E.M.[5], García-Villata J.E..[2], Gonzales Perez A.M.[6], Rios R.[5], Romero K.[4], Sorto V.[4], Mejía Valencia J.G.[6], Combe M.[7], Gozlan R.E.[7†]

[1] EVECO group, Univ. of Antwerp, Antwerp, Belgium
[2] Instituto de Investigaciones Tropicales de El Salvador, El Salvador
[3] Escuela de Medicina Veterinaria, Facultad de Medicina Veterinaria y Agronomia, Universidad de las Americas, Santiago, Chile
[4] Universidad Evangélica de El Salvador (UEES), San Salvador, El Salvador
[5] Facultad de Ciencias Naturales, Universidad de El Salvador (UES), San Salvador, El Salvador
[6] Centro de Investigaciones y Desarrollo en Salud (CENSALUD), Universidad de El Salvador (UES), San Salvador, El Salvador
[7] ISEM, Univ Montpellier, CNRS, IRD, Montpellier, France

*Equally contributing authors

[†] Corresponding authors marina.voinson@uantwerpen.be ; rudy.gozlan@ird.fr

Keywords: Planetary Health, Zoonosis, Food Security, Environmental Change, Conservation

Abstract

Reconciling biodiversity conservation, food security, and human health remains a major sustainability challenge, largely because these dimensions are often examined in isolation. Here, we present an integrated analytical framework that extends coexistence theory by explicitly incorporating zoonotic emergence within a One Health perspective. Using Central America as a case study, we combine spatial indicators of anthropogenic pressure, livestock density, biodiversity, and disease occurrence to identify convergence zones of socio-ecological vulnerability. Our analyses reveal non-linear interactions and asymmetries among coexistence parameters, underscoring that zoonotic emergence arises from constellations of pressures rather than single drivers. We further show how integrated vulnerability mapping can translate this conceptual framework into operational tools, highlighting areas where interventions are likely to yield the greatest co-benefits. Overall, this approach provides a transferable method for identifying leverage points where targeted actions can simultaneously reduce disease risk, strengthen food security, and support biodiversity conservation. By reframing sustainability challenges through an explicitly integrated One Health lens, it offers a practical pathway for guiding policy and land-use strategies toward more resilient socio-ecological systems.

Introduction

Reconciling biodiversity conservation with food security has emerged as one of the defining sustainability challenges of the 21st century. Nowhere is this tension more acute than in Central America, a region simultaneously marked by exceptional biological richness and persistent socioeconomic vulnerability. This region is subject to continually expanding agricultural frontiers, such incursions into some of the globe's most biodiverse regions leave communities vulnerable to endemic food insecurity (Sibrian, et al. 2021), higher zoonotic disease exposure (Jones, et al. 2013) (Tajudeen, et al. 2022), and deficient governance systems (King, et al. 2016) (Xavier, et al. 2022). The convergence of these drivers not only threatens the integrity of the region's ecological system, but it also places it at risk for new and recurring health crises whose impacts extend far beyond national borders. Central America's mosaic of ecosystems, from humid tropical forest to dry corridors, highland cloud forest and large agroecosystems, composes a complex geography of risk. These diverse landscapes share a multitude of biological communities, many of which act as reservoirs for pandemic-capable pathogens. Concurrently, structural disparities in food accessibility, pervasive land degradation, and dependence upon smallholder agriculture increase human exposure to environmental shocks and health risks. Consequently, understanding these biophysical and social interactions is essential for navigating the food-biodiversity challenge (the tradeoff between food security and biodiversity conservation). By integrating a One Health perspective, we can identify pathways to anticipate and mitigate zoonotic risks and spillovers without compromising ecological systems while we ensure sustainable food production and rural livelihoods.

Recent conceptual advances in the study of social-ecological systems offer powerful tools to address this challenge. Building on work that frames agroecological landscapes as dynamic systems capable of existing in alternative states, ranging from conflict to coexistence, researchers have introduced the notion of "*coexistence parameters*" (Crespin et Simonetti 2020), which refers to the social and ecological factors that can be managed to reduce biodiversity impacts or increase tolerance to them, thereby shifting a system toward states where food security and biodiversity can be simultaneously achieved (Jouzi, Leung et Nelson 2022). Expanding on this perspective, Crespin and Moreira-Arce (2026) outline an agroecological systems model of coexistence where food security and biodiversity are

framed as multidimensional axes and their interlocations determine spaces for coexistence . This approach not only integrates ecological and socioeconomic processes but also provides a roadmap for identifying actionable levers in context-specific landscapes. However, the coexistence framework remains underexplored with respect to zoonotic risk (Hirst et Halsey 2023). The ecological and social drivers of coexistence for agriculture and biodiversity conservation can also shape the risk of pathogen emergence (Case, et al. 2022). For example, forest fragmentation can simultaneously reduce ecosystem services, displace wildlife hosts, and increase human exposure to vectors. Likewise, food insecurity can drive practices such as bushmeat hunting or livestock intensification that heighten zoonotic spillover risks (Hayek 2022). In contrast, diversified agroecological systems can buffer the transmission of diseases through the conservation of ecological relations that dilute the prevalence of pathogens, and the delivery of stable, nutritious food supplies. Integrating zoonotic dynamics within the coexistence model thus highlights a key frontier for sustainability science.

Here, we propose to examine the regional diversities of Central America both as a challenge and an opportunity for operationalizing this integrated approach. Despite shared historical trajectories and ecological continuities, each country exhibits distinct combinations of environmental degradation, agricultural practices, governance structures, and health system capacities. These differences shape not only national vulnerabilities but also transboundary dynamics of risk. For example, vector-borne diseases like dengue or chikungunya do not respect political border (Charles, et al. 2021), the same way ecological communities also do not. Also, deforestation in one country may alter disease ecology across a wider region (Ortiz, et al. 2021), mirroring how agricultural deficiencies within one region can spur migration pressures that transform exposure patterns elsewhere (Dodd, et al. 2020). A regional perspective is thus paramount.

Our analysis rests on three interrelated pillars. First, we build on the theoretical framework of coexistence parameters to conceptualize how social-ecological interactions underpin the coupled dynamics of biodiversity, food security, and zoonotic risk. By disaggregating food security into its core components (availability, access, utilization, and stability) and biodiversity into its composition, structure, and function, we can identify specific points of interaction where coexistence (or conflict)

emerges. This multidimensional framing enables us to move beyond simplistic trade-offs to recognize the conditions under which coexistence is both possible and beneficial.

Second, we propose a pragmatic framework grounded in integrated vulnerability mapping. We argue that identifying "socio-ecological vulnerability hotspots" requires superimposing data on biodiversity erosion (e.g., deforestation rates), performance indicators of food insecurity, and disease burdens (Prist, et al. 2023) . This type of mapping provides a spatially explicit tool to locate where risks converge, highlighting where interventions can yield the highest impact. Crucially, this aligns with the One Health paradigm, emphasizing the interdependence of human, animal, and environmental/ecosystem health.

Third, we explore the implications for regional sustainability and governance. Central America's status as a biodiversity hotspot and a global migration corridor means that local risks carry international consequences. By integrating zoonotic dynamics into coexistence models, we offer a novel framework for regional policy forums regarding food safety and accessibility, land use, and health preparedness. Integration is vital as accelerating climate disruption threatens to exacerbate vulnerabilities across the entire food-biodiversity-health nexus (United Nations Environment Programme s.d.).

Ultimately, we bridge the gap between conceptual innovation and applied sustainability research. Whereas much of the literature treats biodiversity conservation, food security, and health as separate agendas, we argue that their nexus (their point of intersection) is precisely where the most transformative opportunities lie. Aligning agroecological transitions with public health strategies and regional food policies allows for the creation of pathways that simultaneously safeguard biodiversity, reduce disease risks, and enhance human well-being. The potential payoffs are considerable. By identifying and managing coexistence parameters to reduce ecological impacts while securing food and health, Central American countries can transition from reactive crisis management towards proactive resilience-building. Moreover, these lessons offer a scalable model for other tropical landscapes where biodiversity, agriculture, and health intersect.

Methods

Study area and data sources

The study was conducted across six Central American countries (Belize, Costa Rica, El Salvador, Guatemala, Honduras, and Nicaragua) forming a biologically rich and environmentally heterogeneous region. This area spans tropical lowlands, intensively cultivated agricultural landscapes, densely populated urban corridors, and mountainous forested ecosystems. The climate is predominantly tropical, with marked wet and dry seasons shaped by altitudinal gradients and the contrasting influences of the Caribbean Sea and the Pacific Ocean. Land use patterns vary widely across the region, ranging from expanding croplands and peri-urban settlements to protected forests and coastal wetlands. This mosaic of ecological and socio-economic conditions creates a dynamic interface between human, livestock, and wildlife populations, making Central America an ideal setting for investigating the environmental drivers of zoonotic disease emergence.

To capture this complexity, the study integrates a broad set of spatially and temporally explicit covariates derived from multiple open-access data sources (see Supplementary Information 1). These include socio-demographic indicators (NASA SEDAC, WCS) (Wildlife Conservation Society 2025) (Center For International Earth Science Information Network-CIESIN-Columbia University 2017), land cover and vegetation metrics (Sentinel-2) (Land Cover 2020 (raster 10 m), global, annual - version 1 2025), dominant crop distributions (MapSPAM) ((IFPRI) et (IIASA) 2015) (International Food Policy Research Institute (IFPRI) 2019) (International Food Policy Research Institute (IFPRI) 2024), livestock densities (Global Livestock of the World) (Gilbert, et al. 2018), climatic variables (NASA POWER) (Sparks 2018), and wildlife richness layers (IUCN 2021). Together, these datasets provide a comprehensive representation of the environmental, agricultural, climatic, and biological gradients shaping disease risk across the region.

Spatial distribution of zoonotic cases were collected from the OMSA-WAHIS database (see supplementary information SI1) and included a total of 21 pathogens over a 21 years period (2005-2025). These data enable a regional assessment of environmental correlates of zoonotic emergence across multiple pathogen systems.

Within this broader comparative framework, we conducted a focused analysis of the New World screwworm fly (*Cochliomyia hominivorax*) as a model parasitic system linking environmental change, host availability, and human activity. All emergence records reported in the OMSA–WAHIS database

and classified as *C. hominivorax* cases were extracted and used to characterize its spatial and environmental distribution across the study region. This species represents a well-suited case for spatial epidemiological analysis due to its strong dependence on climatic conditions, livestock distribution, and land-use patterns, as well as its major veterinary and public health relevance in Central America. Historically targeted by large-scale eradication programs, its recent re-emergence highlights the dynamic and often unpredictable nature of zoonotic threats in rapidly changing landscapes. By modeling the spatial distribution of *C. hominivorax* alongside broader zoonotic disease patterns, we provide a biologically grounded example of how environmental and socio-ecological drivers identified at the regional scale translate into risk for a specific, high-impact parasite affecting livestock systems, food security, and rural livelihoods. Hereafter, we refer to the model built using the full multi-pathogen dataset as the "all-zoonoses model," and to the species-specific analysis based on *C. hominivorax* records as the "*C. hominivorax* model."

Modeling framework

To investigate the spatial and temporal determinants of zoonotic disease occurrence, we implemented a spatial hierarchical model using the Integrated Nested Laplace Approximation (INLA) framework. The analysis was conducted on a regular grid of 10 × 10 km cells covering the study area, providing a consistent spatial unit for integrating outbreak data and environmental covariates. Each grid cell was evaluated for every year of the 21-year study period, producing a complete spatio-temporal panel of cell-year observations used for model fitting.

Reported animal outbreak locations were spatially aggregated within each grid cell and year. For each cell, we computed the number of distinct outbreaks. Cells with no recorded outbreaks were considered as pseudo-absences and retained in the analysis to represent background conditions. This grid-based approach allows accounting for spatial heterogeneity in surveillance intensity and environmental drivers while ensuring comparability across the study area.

Environmental and socio-demographic covariates were extracted for each grid cell by overlaying the spatial layers with the grid. For continuous predictors (e.g., temperature, rainfall, population density, livestock densities, land cover proportions), we computed the mean value within each cell. All covariates

were standardized (z-scores) to ensure comparability of model coefficients and reduce scale-related effects (see Table 1).

Spatial dependence among neighboring cells was modeled using the Stochastic Partial Differential Equation (SPDE) approach implemented in R-INLA, which approximates a continuous spatial random field through a triangular mesh constructed over the study area. Temporal dynamics were incorporated through a yearly random effect (RW1), allowing the model to capture interannual fluctuations in emergence risk across the 21-year period beyond what is explained by fixed covariates. Posterior means and 95% credible intervals were used to quantify the magnitude and uncertainty of associations between covariates and emergence risk.

To avoid multicollinearity, we retained only one representative variable for temperature, precipitation, and wind based on variance inflation factor (VIF) analysis. Mean temperature and precipitation were selected to represent overall climatic conditions, while maximum wind speed was retained to capture gust events relevant to transmission and to limit multicollinearity.

Bayesian spatial negative binomial model. To investigate the spatial determinants of zoonotic disease occurrence, we implemented a Bayesian hierarchical spatial model using the Integrated Nested Laplace Approximation (INLA) framework. The analysis was conducted on a regular grid of 10 × 10 km cells covering the study area, which provided a consistent spatial unit for integrating outbreak data and environmental covariates.

Let Y_i denote the observed number of reported cases in grid cell $i (i = 1, \ldots, N)$. Given the count nature of the data and the presence of overdispersion, Y_i was assumed to follow a negative binomial distribution:

$$Y_i \sim \text{Negative Binomial}(\lambda_i, \kappa),$$

where λ_i is the expected number of cases in grid cell i, and κ is the dispersion parameter accounting for extra-Poisson variability.

The expected number of outbreaks was modeled on the logarithmic scale as:

$$\log(\lambda_i) = \alpha + \sum_{j=1}^{p} \beta_j X_{ij} + r_i + v_i + u(t_i),$$

where α is the intercept, X_{ij}denotes the value of covariate $j$in grid cell i, $\beta_j$are the corresponding regression coefficients, and p is the total number of covariates included in the model.

The term r_i represents an unstructured random effect capturing residual heterogeneity across grid cells, while $v_i$denotes the spatially structured random effect accounting for residual spatial autocorrelation. The spatial effect v_i was modeled as a Gaussian random field with a Matérn covariance structure, estimated using the stochastic partial differential equation (SPDE) approach implemented in *R-INLA*. This approach approximates the continuous spatial field through a triangular mesh constructed over the study area. Finally, $u(t_i)$is the RW1 temporal effect.

Priors for the SPDE range and marginal variance, as well as the RW1 precision, were specified using penalized complexity (PC) priors, which shrink toward simpler (smoother) representations unless strongly supported by the data.

Mesh construction and spatial modeling: The observed number of cases was modeled as a spatially continuous process using Gaussian random fields (GRFs). To account for spatial dependence and overdispersion, we employed a negative binomial regression framework combined with a spatially structured latent field. Spatial effects were incorporated using the stochastic partial differential equation (SPDE) approach implemented in the *R-INLA* package (version 23.04.24), which enables efficient Bayesian inference for latent spatial models.

The SPDE approach provides a continuous representation of the GRF, which is approximated numerically using the finite element method (FEM). In this framework, the spatial domain $D$is discretized into a triangulated mesh, over which the spatial field is represented through basis functions defined at the mesh vertices. The structure and resolution of the mesh play a critical role in accurately capturing spatial autocorrelation while maintaining computational efficiency.

Mesh construction followed a two-step procedure. First, mesh vertices were placed at the sampling locations to ensure adequate resolution of the spatial field in areas with observed data. Additional vertices were subsequently added to cover the entire spatial domain and to support spatial prediction in unsampled regions, including near domain boundaries to reduce edge effects.

An initial spatial range of 400 km was selected as a reasonable scale for representing broad regional patterns of zoonotic emergence across Central America. This distance captures large-scale spatial continuity without over smoothing differences between ecological zones. The maximum edge length in the inner mesh was set to one-fifth of this range (100 km) to ensure sufficient resolution within the study area, following common practical guidelines for SPDE models. For the outer mesh, the maximum edge length was set equal to the assumed spatial range (400 km), creating a buffer that reduces boundary effects and allows the spatial field to taper smoothly.

To evaluate the robustness of this mesh structure, we also constructed models using smaller (100 km) and larger (700 km) spatial ranges, applying the same proportional rules for inner and outer edge lengths. Results across the 100 km, 400 km, and 700 km meshes were highly consistent, confirming that the 400 km configuration provided a balanced and computationally efficient representation of spatial dependence for subsequent inference, with results summarized in Table 3.

Cross-validated predictive performance. We evaluated predictive performance using a 5-fold cross-validation scheme. In each fold, 80% of the data were used for model training and the remaining 20% for testing, allowing assessment on unseen data while preserving the spatial and temporal dependence structure. Predictive performance was first assessed using all recorded emergence events, regardless of etiology, providing a global evaluation of the model's ability to identify areas prone to zoonotic disease emergence.

Because the study also aimed to characterize and predict emergence events specifically attributable to *Cochliomyia hominivorax* (New World screwworm), we additionally repeated the cross-validated evaluation after restricting the test data to emergence observations involving this species only. This species-specific assessment ensures that model performance directly reflects the ability to detect and prioritize high-risk locations for screwworm outbreaks, without being diluted by emergence events arising from unrelated pathogens. Evaluating both the full dataset and the *C. hominivorax* subset therefore provides a comprehensive understanding of the model's behavior: a broad assessment across all etiologies, and a targeted analysis focused on a species of major epidemiological relevance.

For each fold, we computed the log pseudo-marginal likelihood (LPML) derived from the conditional predictive ordinates (CPO), which provides a leave-one-out predictive score. LPML was preferred over

information criteria such as DIC or WAIC because it directly measures out-of-sample predictive accuracy. We summarize results as the mean LPML per observation and its variability across the five folds. In addition, discriminative ability was evaluated on aggregated cross-validated predictions using the Area Under the Receiver Operating Characteristic Curve (AUROC) and the Area Under the Precision–Recall Curve (AUPRC), the latter being particularly appropriate given the extreme rarity of emergence events (in the dataset ≈0.53% of all observations). Both metrics were complemented with bootstrap 95% confidence intervals (2000 bootstraps).

Finally, we evaluated model performance under realistic operational constraints by examining decision thresholds based on ranked risk, rather than absolute predicted probabilities. Surveillance programs typically operate under limited resources and can only inspect a fraction of all locations. Therefore, we reported performance at two interpretable thresholds: Top 1% highest-risk locations (≈10 alerts per 1,000), and Top 5% highest-risk locations (≈50 alerts per 1,000). For each threshold, we computed: True/false positives and negatives (TP, FP, TN, FN), Precision (PPV) and Recall, Lift (PPV divided by the prevalence), True positives per 1,000 inspected units, and bootstrapped 95% CIs.

This workload-centric formulation provides a surveillance-relevant summary of how many emergence events the model can detect for a given inspection effort.

Regression coefficients for fixed covariates were estimated for each model. As INLA is a Bayesian inference framework, results are reported using posterior means and 95% Bayesian credible intervals (BCIs). To facilitate interpretation, we derived relative risks (RRs) by comparing the posterior mean of the expected number of cases at a given covariate value, $\mu(x)$, to that at a reference value, $\mu(\text{ref})$:

$$RR = \frac{\mu(x)}{\mu(\text{ref})}.$$

Conservative 95% BCIs for the relative risks were computed as:

$$RR_{\text{lower}} = \frac{\mu_x^{\text{lower}}}{\mu_{\text{ref}}^{\text{upper}}}, RR_{\text{upper}} = \frac{\mu_x^{\text{upper}}}{\mu_{\text{ref}}^{\text{lower}}}.$$

An association was considered statistically significant when the 95% Bayesian credible interval (BCI) of the regression coefficient did not include zero and the corresponding 95% BCI of the relative risk did not include one.

Results

Model performance was evaluated separately for two complementary modeling frameworks: (i) the all-zoonoses model, which integrates emergence data across all pathogens to identify broad environmental drivers of zoonotic risk, and (ii) the *C. hominivorax* model, a species-specific analysis designed to capture the ecological and livestock-related determinants of emergence for this focal parasite.

For the all-zoonoses framework, model performance was compared across spatial configurations using neighborhood radii of 100, 400, and 700 km, with year included as a fixed covariate in all cases (Table 2). Across these scales, predictive performance was highly consistent, with comparable LPML and discrimination metrics (AUROC ≈ 0.89; AUPRC ≈ 0.12). The 400 km spatial configuration was selected for inference, as it provided the most stable LPML estimate and represented a balanced spatial structure for capturing regional continuity in zoonotic emergence. This model is used to infer general environmental and socio-ecological drivers of zoonotic risk across pathogens.

For *C. hominivorax*, predictive performance improved markedly when cattle density was modeled as a non-linear RW2 effect. The 400 km RW2 model achieved the highest predictive accuracy among all species-specific configurations (AUROC = 0.97–0.98; AUPRC = 0.26), reflecting its ability to capture the sharp density-dependent patterns underlying screwworm emergence. Because this model was fitted to a restricted dataset of laboratory-confirmed cases, its LPML values are not directly comparable to those of the all-zoonoses models; however, its high discrimination metrics indicate excellent predictive performance for this pathogen.

Together, these models serve complementary purposes: the all-zoonoses model identifies generalizable drivers of zoonotic emergence at the regional scale, while the *C. hominivorax* model provides a biologically grounded, pathogen-specific assessment of how these drivers translate into risk for a high-impact parasitic system. All subsequent analyses—including fixed-effect estimates, spatial risk maps, and temporal patterns—are therefore based on the selected 400 km configurations for each modeling framework.

Fixed covariates

Fixed covariates analysis revealed that climatic and ecological factors were the strongest predictors of zoonotic disease emergence across livestock systems, whereas socio-demographic and most land-cover variables displayed weak or uncertain effects (Table 3-4). In the all-zoonoses model, temperature showed a clear negative association with emergence risk (posterior mean = −0.35; RR = 0.71, 95% BCI: 0.68–0.74), indicating reduced suitability in cooler environments. Precipitation exhibited a strong positive effect (posterior mean = 0.25; RR = 1.29, 95% BCI: 1.18–1.41), suggesting that wetter conditions promote environmental suitability for a broad set of zoonotic pathogens or vectors. Wind speed had a weak and uncertain effect (posterior mean = 0.05; RR = 1.05, 95% BCI: 0.82–1.36). Mammal–bird richness was strongly and positively associated with emergence risk (posterior mean = 0.76; RR = 2.13, 95% BCI: 1.43–3.18), highlighting the role of diverse wildlife communities in sustaining reservoir host availability and pathogen circulation. Among anthropogenic variables, cropland showed a modest negative association (posterior mean = −0.21; RR = 0.81, 95% BCI: 0.67–0.97), while built-up and water areas showed non-significant effects. Human population density did not influence emergence risk (posterior mean = −0.08; RR = 0.92, 95% BCI: 0.78–1.10), but the Human Footprint Index displayed a strong positive association (posterior mean = 0.78; RR = 2.19, 95% BCI: 1.61–2.99), suggesting that human-modified landscapes may indirectly facilitate zoonotic spillover or detection through intensified livestock–wildlife interactions or surveillance biases.

The pathogen-specific *C. hominivorax* model (see Table 4) exhibited broadly similar patterns but with stronger effect sizes for several key covariates. Temperature had a more pronounced negative effect (posterior mean = −0.55; RR = 0.57, 95% BCI: 0.53–0.62), consistent with the species' requirement for warm environments for larval development and adult activity. Precipitation also showed a stronger positive association (posterior mean = 0.28; RR = 1.32, 95% BCI: 1.18–1.49), reinforcing the importance of humid conditions for this obligate parasitic fly. Mammal–bird richness had an even stronger effect in the *C. hominivorax* model (posterior mean = 1.01; RR = 2.75, 95% BCI: 1.52–5.06), suggesting heightened sensitivity to host community structure. In contrast, socio-demographic and land-cover variables generally showed weak or uncertain effects, with the exception of cropland, which retained a negative association (posterior mean = −0.23; RR = 0.79, 95% BCI: 0.63–0.99). The Human

Footprint Index also showed a positive but more moderate effect (posterior mean = 0.59; RR = 1.81, 95% BCI: 1.14–2.88).

Across both models, warm temperatures, high precipitation, and rich wildlife communities emerged as the dominant drivers of zoonotic risk, though the species-specific model for *C. hominivorax* showed sharper and more pronounced effect sizes. This pattern suggests that while general environmental suitability governs broad zoonotic emergence processes, *C. hominivorax* responds more strongly to climatic and ecological gradients, reflecting its biology as a highly temperature-dependent, host-seeking parasitic fly.

Identifying emergence risk

Across the study region, both the all-zoonotic emergence model and the *Cochliomyia hominivorax*–specific model revealed similar large-scale spatial patterns, with elevated mean emergence risk concentrated in southern Mexico, Guatemala, Honduras, and Nicaragua (Figure 1–2). For both outcomes, these high-risk zones coincided with areas of low spatial uncertainty and narrow 95% credible intervals, indicating strong model support. However, notable differences emerged in the spatial extent and sharpness of the predicted hotspots. The all-zoonoses model produced a broader distribution of elevated risk and greater uncertainty in peripheral areas, whereas the *C. hominivorax* model yielded more spatially focused hotspots with clearer boundaries, reflecting a stronger and more localized signal in pathogen-specific emergence events. In both models, combining predicted risk with uncertainty identified reliable hotspots in southern Mexico and northern Central America, as well as uncertain hotspots in regions where elevated risk was accompanied by wider credible intervals. Areas outside these hotspots showed low predicted emergence risk and limited spatial structure. These spatial patterns are consistent with the performance profiles obtained from threshold-based classifications (Table S1), where the top 1% risk cutoff identified a small set of high-precision hotspots, while the broader top 5% cutoff captured more diffuse but less certain emergence signals.

Non-linear trends in cattle density: livestock emergence risk exhibited a pronounced non-linear relationship with cattle density across all models (Figure 3). When considering all reported zoonotic

events collectively (Figure 3A), the posterior effect rose steeply at low cattle densities and reached a maximum at intermediate densities (approximately 80,000–100,000 animals). Beyond this point, the predicted emergence risk declined steadily, accompanied by wider credible intervals reflecting increased uncertainty in areas with very high cattle concentrations. The pattern was stronger when focusing specifically on emergence events associated with *Cochliomyia hominivorax* (Figure 3B). In this pathogen-specific model, the rise toward the peak was sharper and the subsequent decline at high densities was more pronounced, suggesting a heightened density-dependent response for this particular zoonotic agent. Overall, these results indicate that intermediate cattle densities are most strongly associated with elevated emergence risk, while both sparse and extremely dense livestock systems exhibit substantially lower likelihoods of zoonotic disease occurrence.

Temporal effect

Temporal patterns revealed contrasting emergence dynamics between the all-zoonoses model and the *C. hominivorax*–specific model (Figure 4). In the all-zoonoses model (Figure 4A), the temporal random effect displayed moderate year-to-year variability but followed a broadly increasing trajectory across the study period. After a low baseline around 2006–2008, the effect rose steadily with small oscillations, and a marked acceleration appeared after 2020, when the posterior mean increased sharply and credible intervals narrowed. This consistent upward trend indicates a gradual intensification of zoonotic emergence processes in livestock, potentially driven by long-term environmental shifts, expanding livestock–wildlife interfaces, and enhanced detection capacity.

In contrast, the *C. hominivorax* model (Figure 4B) showed a markedly different temporal structure reflecting the species' near-absence in Central America before its recent resurgence. From 2005 through approximately 2018, the temporal random effect remained close to zero with wide credible intervals—patterns consistent with very few or no recorded cases, corresponding to the near-extinction of *C. hominivorax* from Central America during this period. A slight fluctuation occurred around 2010, but overall the trajectory remained flat and uncertain until the late 2010s. Beginning around 2018–2020, the temporal effect increased abruptly, followed by an exceptionally sharp rise in the final years of the series, accompanied by narrowing credible intervals. This pattern indicates the emergence of a robust

393 and well-supported signal of re-establishment or spread, aligning with field observations of renewed *C.*
394 *hominivorax* detections after a prolonged period of regional disappearance.
395 Taken together, these results show that while all-zoonoses emergence increased gradually over time, *C.*
396 *hominivorax* displays a distinct signature characterized by near-absence for more than a decade,
397 followed by a sudden and rapid increase in emergence probability. This contrast underscores the value
398 of species-specific models in distinguishing broad epidemiological trends from pathogen-specific
399 resurgence dynamics.
400

401 ## Discussion

402 Our results provide empirical support for the conceptual expansion of the food-biodiversity nexus, which
403 now frames biodiversity, food security, and health as interdependent dimensions of a single coexistence
404 nexus rather than as parallel or competing policy domains (König, et al. 2020), (Fiasco et Massarella
405 2022) (Massarella, et al. 2022). By integrating zoonotic emergence into the agroecological systems
406 model of coexistence, this study moves beyond trade-off narratives and demonstrates that the drivers
407 shaping food-biodiversity relations also dictate the geography of health risk in Central America.
408 Across the region, zoonotic risk did not appear randomly scattered across the landscape. Instead, it
409 tended to concentrate in specific places where human activity, livestock presence, and wildlife diversity
410 overlap. The consistent links we observed between the Human Footprint Index, cattle density, and
411 mammal and bird richness point to these human-animal-environment interfaces as recurring sites where
412 emergence is more likely to occur (Mancini, et al. 2024) (Palmeirim, Barreto et Prist 2025). In practice,
413 these areas correspond closely to what we describe in Box 1 as the animal health and environmental
414 health dimensions of the One Health axis. Where livestock systems are intensified, the number of
415 potential hosts and contacts inevitably increases (Perfecto, et al. 2023) (Klous, et al. 2016). At the same
416 time, biodiverse landscapes can act as long-term reservoirs in which pathogens persist and circulate.
417 Together, these processes define a subset of the coexistence niche where food production, biodiversity
418 conservation, and health risks intersect most sharply.

Importantly, our findings also reveal asymmetries among coexistence parameters. Some pressures clearly push systems in one direction, while others seem to work in the opposite sense. This divergence is particularly evident in the opposing roles of landscape pressure and agricultural management. While intensified human activity (captures by the Human Footprint Index) acts as a primary destabilizer by more than doubling zoonotic risk (RR = 2.19), not all anthropogenic modifications lead to the same outcome. In contrast, specific agricultural configurations like cropland cover appear to offer a modest buffer (RR = 0.81), suggesting that the 'quality' of land use, rather than just its extent, determines the system's trajectory. This dynamic is further complicated by a 'biodiversity paradox' that we observe in the region: while mammal and bird richness remains a primary conservation objective, it inherently increases emergence risk (RR = 2.13) by sustaining the reservoir communities required for pathogen circulation.

Navigating these contradictory forces is essential for identifying the precise leverage points (such as managing land-use intensity and livestock density thresholds) needed to nudge a landscape toward a stable basin of coexistence. Ultimately, acknowledging these asymmetries allows for a more proactive approach to transboundary health security, ensuring that a regional development does not inadvertently trigger the next spillover event.

What also stands out is how little explanatory power some land-use or crop-specific variables seem to carry on their own. This suggests that zoonotic emergence is probably not something that can be traced back to a single cause or pressure (Chaves, et al. 2022). In practice, emergence originates through particular constellations of factors acting concurrently, sometimes subtly, across scales (Jagadesh, Combe et Gozlan 2022). Viewing the system through this lens reveals coexistence not as a static outcome, but as dynamic position within a complex, multidimensional space (Combs, et al. 2021) (Crespin et Simonetti 2020). Local systems may drift, gradually or abruptly, toward more stable or more fragile states. From this angle, zoonotic outbreaks are less an anomaly than a signal, a sign that accumulated pressures on animal and environmental health are beginning to spill over, with consequences for food security and the system's ability to absorb future shocks (Perfecto, et al. 2023).

The cattle sector plays a pivotal role in the economies of numerous Latin American and Caribbean countries, and our results show that cattle density is also a key ecological and epidemiological

447 determinant of emergence risk in the region (Sandoval, et al. 2024). In both models, risk increased
448 sharply at low to intermediate cattle densities and then declined at higher densities, but the pattern was
449 far steeper and more tightly structured for *C. hominivorax*. This species-specific response is consistent
450 with its biology as an obligate parasitic fly that depends on the availability of warm-blooded hosts for
451 larval development (Long, et al. 2026). At intermediate densities, livestock abundance and management
452 practices likely create favorable conditions for wound exposure, host attraction, and fly reproduction,
453 producing a clear peak in predicted risk. At very high densities, however, the predicted decline in risk
454 may reflect the shift toward more intensive production systems, where improved animal handling,
455 wound care, and vector control reduce opportunities for infestation. The all-zoonoses model showed the
456 same overall hump-shaped pattern, but with a shallower slope and broader uncertainty, suggesting that
457 the strong density dependence observed for *C. hominivorax* is a major contributor to the general
458 emergence signal. Together, these results indicate that cattle density is not simply a linear driver of
459 disease risk, but a factor whose influence is shaped by host availability, husbandry practices, and the
460 ecological requirements of *C. hominivorax*, which remains a key component of the broader zoonotic
461 emergence landscape.
462 Temporal dynamics reinforce this interpretation. The all-zoonoses model displayed a gradual regional
463 increase over time, whereas the *C. hominivorax* model showed near-absence for more than a decade
464 followed by a sharp resurgence after 2018–2020—consistent with historical near-eradication and
465 renewed expansion in Central America (Valdez-Espinoza, et al. 2025). These patterns underscore that
466 coexistence is inherently dynamic. Even without dramatic land-use changes, shifts in climate, pathogen
467 movement, or surveillance intensity can progressively erode system stability (Mulieri et Patitucci 2019).
468 From a One Health perspective, temporal early-warning indicators may therefore be as critical as spatial
469 hotspot detection in anticipating future crises.
470 By operationalizing the coexistence nexus through integrated vulnerability mapping, our approach
471 provides a concrete pathway for translating theory into action. Overlaying biodiversity erosion, food
472 insecurity indicators, and zoonotic risk allows the identification of socio-ecological hotspots where
473 targeted interventions are likely to yield the greatest benefits. In these areas, managing a small number
474 of key coexistence parameters (such as livestock density, landscape connectivity, or forest cover) could

simultaneously reduce disease risk, enhance food stability, and preserve biodiversity (Prist, et al. 2023) (Mancini, et al. 2024).

At the policy level, the results argue strongly against uniform surveillance or disease-management strategies (Combs, et al. 2021). The risk maps clearly show that zoonotic emergence is highly spatially clustered, with reliable hotspots concentrated in southern Mexico and northern Central America, and large surrounding areas displaying consistently low or highly uncertain risk. This spatial heterogeneity means that blanket interventions would be inefficient and potentially waste limited resources. Instead, the mapped patterns of mean risk, uncertainty, and hotspot classification point toward context-specific interventions tailored to the local configuration of coexistence pressures. Aligning agricultural, environmental, and public health policies—particularly through coordinated cross-ministerial planning—can help embed disease-mitigation strategies within broader sustainability agendas, rather than treating zoonotic emergence as an episodic crisis requiring reactive responses (Clifford Astbury, et al. 2023). In practice, this implies prioritizing intensified surveillance and preventive measures in reliable hotspots, strengthening environmental buffers in uncertain zones, and adopting lighter-touch strategies in low-risk areas.

More broadly, Central America provides a compelling illustration of how local drivers (environmental degradation, agricultural practices, and socioeconomic vulnerability) can generate risks with regional and global implications (Obura, et al. 2021). While the specific coexistence parameters identified here are context-dependent, the underlying framework is transferable (Mahon, et al. 2024). Applying the coexistence nexus to other tropical and subtropical regions could help uncover generalizable trajectories of zoonotic emergence, even when the proximate drivers remain locally specific.

To conclude, this study demonstrates that the food–biodiversity challenge cannot be addressed without explicitly integrating a One Health perspective. Moving beyond a two-dimensional trade-off between production and conservation, we propose a three-dimensional coexistence framework in which environmental health underpins both human well-being and disease prevention. Our findings from Central America show that socio-ecological vulnerability hotspots are not inevitable outcomes, but emerge from specific interactions among agricultural expansion, biodiversity loss, and governance gaps.

Identifying and managing key coexistence parameters—particularly thresholds in human footprint and livestock density—offers a proactive pathway toward regional resilience. As climate disruption accelerates, this integrated framework provides a scalable approach for other tropical regions facing the competing demands of food production, biodiversity conservation, and public health. Sustainability, therefore, is not simply about balancing food and nature; it is about safeguarding the conditions of coexistence that sustain ecosystem integrity, livelihoods, and health.

Acknowledgments: S. Crespin was supported by the One Health Community of Knowledge from IRD. M. Voinson, R. Gozlan and M. Combe were supported by the BCOMING project (Horizon Europe project 101059483) from the European Union and FNRS.

References

(IFPRI), International Food Policy Research Institute, and International Institute For Applied Systems Analysis (IIASA). "Global Spatially-Disaggregated Crop Production Statistics Data for 2005 Version 3.2." *Geospatial Data* (Harvard Dataverse), 2015.

Adisasmito, Wiku B., et al. "One Health: A new definition for a sustainable and healthy future." Edited by Jeffrey D. Dvorin. *PLOS Pathogens* (Public Library of Science (PLoS)) 18 (June 2022): e1010537.

Adisasmito, Wiku B., et al. "One Health: A new definition for a sustainable and healthy future." Edited by Jeffrey D. Dvorin. *PLOS Pathogens* (Public Library of Science (PLoS)) 18 (June 2022): e1010537.

Barrera, N. "The Transnational Capture and Pillage of Central America. Jus Semper Global Alliance." *The Transnational Capture and Pillage of Central America. Jus Semper Global Alliance*. 2024.

Case, B. K. M., Jean-Gabriel Young, Daniel Penados, Carlota Monroy, Laurent Hébert-Dufresne, and Lori Stevens. "Spatial epidemiology and adaptive targeted sampling to manage the Chagas disease vector Triatoma dimidiata." Edited by Marilia Sá Carvalho. *PLOS Neglected Tropical Diseases* (Public Library of Science (PLoS)) 16 (June 2022): e0010436.

Center For International Earth Science Information Network-CIESIN-Columbia University. "Gridded Population of the World, Version 4 (GPWv4): Population Density, Revision 11." (Palisades, NY: NASA Socioeconomic Data and Applications Center (SEDAC)) 2017.

Charles, Roxanne A., et al. "Ticks and Tick-Borne Diseases in Central America and the Caribbean: A One Health Perspective." *Pathogens* (MDPI AG) 10 (October 2021): 1273.

Chaves, Luis Fernando, Julie Velasquez Runk, Luke R. Bergmann, and Nicole L. Gottdenker. "Reifications in Disease Ecology 1: Demystifying Land Use Change in Pathogen Emergence." *Capitalism Nature Socialism* (Informa UK Limited) 34 (November 2022): 23–39.

539 Clifford Astbury, Chloe, et al. "Policies to prevent zoonotic spillover: a systematic scoping review
540 of evaluative evidence." *Globalization and Health* (Springer Science and Business Media
541 LLC) 19 (November 2023).
542 Combe, Marine, and Rodolphe Elie Gozlan. "When the Blue Marble Health concept challenges
543 our current understanding of One Health." *One Health* (Elsevier BV) 19 (December 2024):
544 100935.
545 Combs, Matthew A., et al. "Socio-ecological drivers of multiple zoonotic hazards in highly
546 urbanized cities." *Global Change Biology* (Wiley) 28 (December 2021): 1705–1724.
547 Crespin, Silvio J., and Javier A. Simonetti. "Traversing the food-biodiversity nexus towards
548 coexistence by manipulating social–ecological system parameters." *Conservation*
549 *Letters* (Wiley) 14 (November 2020).
550 Crespin, Silvio, and Dario Moreira-Arce. "Creating opportunities for coexistence to overcome the
551 food–biodiversity challenge." (California Digital Library (CDL)) February 2026.
552 Díaz, Sandra, et al. "Assessing nature's contributions to people." *Science* (American Association
553 for the Advancement of Science (AAAS)) 359 (January 2018): 270–272.
554 Dodd, Warren, et al. "Factors Associated with Seasonal Food Insecurity among Small-Scale
555 Subsistence Farming Households in Rural Honduras." *International Journal of*
556 *Environmental Research and Public Health* (MDPI AG) 17 (January 2020): 706.
557 Fiasco, Valentina, and Kate Massarella. "Human-Wildlife Coexistence: Business as Usual
558 Conservation or an Opportunity for Transformative Change?" *Conservation and Society*
559 (Medknow) 20 (April 2022): 167–178.
560 Fischer, Joern, et al. "Reframing the Food–Biodiversity Challenge." *Trends in Ecology &*
561 *Evolution* (Elsevier BV) 32 (May 2017): 335–345.
562 Gilbert, Marius, et al. "Global distribution data for cattle, buffaloes, horses, sheep, goats, pigs,
563 chickens and ducks in 2010." *Scientific Data* (Springer Science and Business Media LLC)
564 5 (October 2018).
565 Hayek, Matthew N. "The infectious disease trap of animal agriculture." *Science Advances*
566 (American Association for the Advancement of Science (AAAS)) 8 (November 2022).
567 Hirst, Kristen M., and Samniqueka J. Halsey. "Bacterial zoonoses impacts to conservation of
568 wildlife populations: a global synthesis." *Frontiers in Conservation Science* (Frontiers
569 Media SA) 4 (November 2023).
570 International Food Policy Research Institute (IFPRI). "Global Spatially-Disaggregated Crop
571 Production Statistics Data for 2010 Version 2.0." *Geospatial Data* (Harvard Dataverse),
572 2019.
573 International Food Policy Research Institute (IFPRI). "Global Spatially-Disaggregated Crop
574 Production Statistics Data for 2020 Version 2.0." *Geospatial Data* (Harvard Dataverse),
575 2024.
576 IUCN, red list. "Species richness of mammals and birds combined with AoH maps." *Species*
577 *richness of mammals and birds combined with AoH maps*. 2021.
578 Jagadesh, Soushieta, Marine Combe, and Rodolphe Elie Gozlan. "Human-Altered Landscapes
579 and Climate to Predict Human Infectious Disease Hotspots." *Tropical Medicine and*
580 *Infectious Disease* (MDPI AG) 7 (July 2022): 124.
581 Jones, Bryony A., et al. "Zoonosis emergence linked to agricultural intensification and
582 environmental change." *Proceedings of the National Academy of Sciences* (Proceedings
583 of the National Academy of Sciences) 110 (May 2013): 8399–8404.
584 Jouzi, Zeynab, Yu-Fai Leung, and Stacy Nelson. "Addressing the food security and conservation
585 challenges: Can be aligned instead of apposed?" *Frontiers in Conservation Science*
586 (Frontiers Media SA) 3 (July 2022).

King, Matthew Wilburn, Marco Antonio González Pastora, Mauricio Castro Salazar, and Carlos Manuel Rodriguez. "Environmental governance and peacebuilding in post-conflict Central America: Lessons from the Central American Commission for Environment and Development." (Routledge) April 2016: 777–802.

Klous, Gijs, Anke Huss, Dick J. J. Heederik, and Roel A. Coutinho. "Human–livestock contacts and their relationship to transmission of zoonotic pathogens, a systematic review of literature." *One Health* (Elsevier BV) 2 (December 2016): 65–76.

König, Hannes J., Christian Kiffner, Stephanie Kramer-Schadt, Christine Fürst, Oliver Keuling, and Adam T. Ford. "Human–wildlife coexistence in a changing world." *Conservation Biology* (Wiley) 34 (May 2020): 786–794.

Long, Brit, Anissa Finley, Stephen Y. Liang, and Heather A. Heaton. "New world screwworm: A focused review for the emergency medicine clinician." *The American Journal of Emergency Medicine* (Elsevier BV) 102 (April 2026): 8–12.

Mahon, Michael B., et al. "A meta-analysis on global change drivers and the risk of infectious disease." *Nature* (Springer Science and Business Media LLC) 629 (May 2024): 830–836.

Mancini, Matheus C. S., Julia Rodrigues Barreto, Raquel L. Carvalho, Renata L. Muylaert, Ricardo Corasa Arrais, and Paula R. Prist. "Landscape Ecology Meets Disease Ecology in the Tropical America: Patterns, Trends, and Future Directions." *Current Landscape Ecology Reports* (Springer Science and Business Media LLC) 9 (April 2024): 31–62.

Massarella, Kate, Judith E. Krauss, Wilhelm Kiwango, and Robert Fletcher. "Exploring Convivial Conservation in Theory and Practice: Possibilities and Challenges for a Transformative Approach to Biodiversity Conservation." *Conservation and Society* (Medknow) 20 (April 2022): 59–68.

Morand, Serge, and Claire Lajaunie. "Outbreaks of Vector-Borne and Zoonotic Diseases Are Associated With Changes in Forest Cover and Oil Palm Expansion at Global Scale." *Frontiers in Veterinary Science* (Frontiers Media SA) 8 (March 2021).

Morris, Aaron L., et al. "Deforestation-driven food-web collapse linked to emerging tropical infectious disease, Mycobacterium ulcerans." *Science Advances* (American Association for the Advancement of Science (AAAS)) 2 (December 2016).

Mulieri, Pablo Ricardo, and Luciano Damián Patitucci. "Using ecological niche models to describe the geographical distribution of the myiasis-causing Cochliomyia hominivorax (Diptera: Calliphoridae) in southern South America." *Parasitology Research* (Springer Science and Business Media LLC) 118 (February 2019): 1077–1086.

Obura, David O., et al. "Integrate biodiversity targets from local to global levels." *Science* (American Association for the Advancement of Science (AAAS)) 373 (August 2021): 746–748.

Ortiz, Diana I., Marta Piche-Ovares, Luis M. Romero-Vega, Joseph Wagman, and Adriana Troyo. "The Impact of Deforestation, Urbanization, and Changing Land Use Patterns on the Ecology of Mosquito and Tick-Borne Diseases in Central America." *Insects* (MDPI AG) 13 (December 2021): 20.

Palmeirim, Ana Filipa, Julia Rodrigues Barreto, and Paula R. Prist. "The importance of Indigenous Lands and landscape structure in shaping the zoonotic disease risk—Insights from the Brazilian Atlantic Forest." *One Health* (Elsevier BV) 21 (December 2025): 101104.

Perfecto, Ivette, et al. "Looking beyond land-use and land-cover change: Zoonoses emerge in the agricultural matrix." *One Earth* (Elsevier BV) 6 (September 2023): 1131–1142.

Prist, Paula Ribeiro, et al. "Promoting landscapes with a low zoonotic disease risk through forest restoration: The need for comprehensive guidelines." *Journal of Applied Ecology* (Wiley) 60 (June 2023): 1510–1521.

Sandoval, Danny Fernando, John Jairo Junca Paredes, Karen Johanna Enciso Valencia, Manuel Francisco Díaz Baca, Aura María Bravo Parra, and Stefan Burkart. "Long-term relationships of beef and dairy cattle and greenhouse gas emissions: Application of co-integrated panel models for Latin America." *Heliyon* (Elsevier BV) 10 (January 2024): e23364.

Service, Copernicus Land Monitoring, and Copernicus Land Monitoring Service Helpdesk. "Land Cover 2020 (raster 10 m), global, annual - version 1." (Copernicus Land Monitoring Service) 2025.

Sibrian, Ricardo, Marco d'Errico, Patricia Palma de Fulladolsa, and Flavia Benedetti-Michelangeli. "Household Resilience to Food and Nutrition Insecurity in Central America and the Caribbean." *Sustainability* (MDPI AG) 13 (August 2021): 9086.

Simon, Sabrina Soares, Marcos Amaku, and Eduardo Massad. "The spread of infectious diseases in migration routes between caravans and resident communities: Modelling yellow fever in Central America." *The Journal of Climate Change and Health* (Elsevier BV) 24 (July 2025): 100473.

Sparks, Adam. "nasapower: A NASA POWER Global Meteorology, Surface Solar Energy and Climatology Data Client for R." *Journal of Open Source Software* (The Open Journal) 3 (October 2018): 1035.

Tajudeen, Yusuf Amuda, Iyiola Olatunji Oladunjoye, Ousman Bajinka, and Habeebullah Jayeola Oladipo. "Zoonotic Spillover in an Era of Rapid Deforestation of Tropical Areas and Unprecedented Wildlife Trafficking: Into the Wild." *Challenges* (MDPI AG) 13 (August 2022): 41.

United Nations Environment Programme, (UNEP). "Helping farmers beat the climate crisis in Central America's Dry Corridor." *Helping farmers beat the climate crisis in Central America's Dry Corridor*. n.d.

Valdez-Espinoza, Uriel Mauricio, Lucas A. Fadda, Roberta Marques, Luis Osorio-Olvera, Daniel Jiménez-García, and Andrés Lira-Noriega. "The reemergence of the New World screwworm and its potential distribution in North America." *Scientific Reports* (Springer Science and Business Media LLC) 15 (July 2025).

WHO. "One Health High-Level Expert Panel Annual Report." Tech. rep., WHO, 2022.

Wildlife Conservation Society. *Human foot print*. 2025. https://wcshumanfootprint.org/data-access.

Xavier, Luciana Yokoyama, Maila Guilhon, Leandra Regina Gonçalves, Marina Ribeiro Corrêa, and Alexander Turra. "Waves of Change: Towards Ecosystem-Based Management to Climate Change Adaptation." *Sustainability* (MDPI AG) 14 (January 2022): 1317.

672 **Table 1**: Standardized covariates used in the model including mean, quartiles, Median and variance
673 inflation factor (VIF).
674

	Covariate	Mean	Q2.5%	Q97.5%	Median	VIF value
Socio-demographic (From NASA SEDAC's and WCS)	Population density (persons/km2)	0.001	-0.305	-0.003	-0.201	1.801
	HFI (/10km)	-0.025	-0.756	0.533	-0.053	2.882
Land cover area (from sentinel 2)	Forest (Ha)	-0.051	-0.473	-0.089	-0.373	1.294
	Water (Ha)	0.009	-0.201	-0.176	-0.199	1.309
	Built up (Ha)	-0.018	-0.557	0.131	-0.339	2.543
	Crops (Ha)	-0.016	-0.267	-0.252	-0.267	1.883
Dominant crops (from MapSPAM)	Banana (Ha)	-0.016	-0.135	-0.131	-0.135	1.204
	Beans (Ha)	0.055	-0.516	0.086	-0.390	1.369
	Maize (Ha)	0.059	-0.488	0.110	-0.315	1.785
	Coconut (Ha)	0.003	-0.140	-0.029	-0.140	1.054
	Palm Oil (Ha)	-0.009	-0.288	-0.195	-0.288	1.237
	Rice (Ha)	-0.026	-0.175	-0.161	-0.174	1.308
	Sugar cane (Ha)	0.009	-0.206	-0.152	-0.203	2.072
Livestock's (from Global Livestock of the World, GLW)	Cattle (Nb/10km)	0.017	-0.714	0.386	-0.258	1.431
	Chicken (Nb/10km)	-0.007	-0.279	-0.042	-0.223	1.398
	Sheep (Nb/10km)	0.014	-0.111	-0.073	-0.097	1.960
	Goat (Nb/10km)	0.025	-0.297	0.000	-0.180	2.224
	Pig (Nb/10km)	0.004	-0.156	-0.043	-0.113	1.206
Climatic variables (from Nasa Power)	Temperature (◦C)	0.000	-0.609	0.755	0.213	1.771
	Precipitation (mm)	0.000	-0.739	0.736	-0.299	1.485
	Wind speed (knots)	0.000	-0.831	0.555	-0.166	1.804
Wild animal richness	Mammal bird richness	-0.052	-0.645	0.624	0.132	1.635

675
676

Table 2: Comparison of spatial model performance based on the logarithmic pseudo-marginal likelihood (LPML) and predictive accuracy metrics. For each model, LPML, AUROC, and AUPRC values are reported as medians with their associated ranges across repeated model fits. All-zoonoses models were fitted using neighborhood radii of 100, 400, and 700 km to assess sensitivity to spatial structure. The *C. hominivorax* models were fitted on a subsampled dataset restricted to confirmed *C. hominivorax* cases and are therefore not directly comparable to the all-zoonoses models. Two specifications are shown: one including cattle density as a fixed effect, and one modelling cattle density using a non-linear RW2 effect.

MODEL	LPML	AUROC (IC 95)	AUPRC (IC 95)	PREVALENCE
ALL-ZOONOTIC 400	**-0.03** (0.0008)	**0.89** (0.88 ; 0.91)	**0.12** (0.10 ; 0.14)	**0.53**
ALL-ZOONOTIC 100	**-0.03** (0.0008)	**0.89** (0.87 ; 0.91)	**0.12** (0.10 ; 0.15)	**0.53**
ALL-ZOONOTIC 700	**-0.03** (0.0008)	**0.89** (0.87 ; 0.91)	**0.12** (0.10 ; 0.15)	**0.53**
***C.HOMINIVIRAX* (+ CATTLE FIXED EFFECT)**	**-0.03** (0.02)	**0.96** (0.96 ; 0.97)	**0.12** (0.10 ; 0.16)	**0.38**
***C.HOMINIVIRAX* (+ CATTLE RW2 EFFECT)**	**-0.017 (0.0004)**	**0.98 (0.97 ; 0.98)**	**0.26 (0.23 ; 0.30)**	**0.38**

Table 3: Posterior mean estimates, 95% Bayesian credible intervals (BCI), and corresponding relative risks (RR) for socio-demographic, land-cover, livestock, climatic, and wildlife covariates included in the final spatial model. Relative risks were obtained by exponentiating posterior mean coefficients and represent the multiplicative change in prevalence associated with a one-unit increase in each standardized covariate, holding all other variables constant. Covariates were classified as having a positive or negative effect when their 95% BCI did not overlap zero (or RR did not overlap 1); effects were considered non-significant otherwise.

	Covariate	***Posterior mean***	***Q025***	***Q975***	***RR (95% BCI)***	***Significative effect***
Socio-demographic	Population density	-0.08	-0.25	0.09	0.92 (0.78 ; 1.10)	-
	HFI	**0.78**	**0.48**	**1.09**	**2.19 (1.61 ; 2.99)**	**Positive**
Land cover area	Built up	-0.06	-0.31	0.19	0.94 (0.73 ; 1.21)	-
	Cropland	**-0.21**	**-0.40**	**-0.02**	**0.81 (0.67 ; 0.97)**	**Negative**
	Water	-0.17	-0.40	0.05	0.84 (0.67 ; 1.05)	-
Climatic variables	**Temperature**	**-0.35**	**-0.39**	**-0.30**	**0.71 (0.68 ; 0.74)**	**Negative**
	Precipitation	**0.25**	**0.17**	**0.34**	**1.29 (1.18 ; 1.41)**	**Positive**
	Wind speed	0.05	-0.20	0.31	1.05 (0.82 ; 1.36)	-
Wild animal richness	**Mammal-bird richness**	**0.76**	**0.36**	**1.16**	**2.13 (1.43 ; 3.18)**	**Positive**

Table 4: Posterior mean estimates, 95% Bayesian credible intervals (BCI), and corresponding relative risks (RR) for socio-demographic, land-cover, livestock, climatic, and wildlife covariates included in the final spatial model for the *C. hominivorax* case study. Relative risks were obtained by exponentiating posterior mean coefficients and represent the multiplicative change in prevalence associated with a one-unit increase in each standardized covariate, holding all other variables constant. Covariates were classified as having a positive or negative effect when their 95% BCI did not overlap zero (or RR did not overlap 1); effects were considered non-significant otherwise.

	Covariate	***Posterior Mean***	***Q025***	***Q975***	***RR (95% BCI)***	***Significative effect***
Socio-demographic	Population density	-0.24	-0.59	0.03	0.79 (0.55 ; 1.12)	-
	HFI	**0.59**	**0.13**	**1.06**	**1.81 (1.14 ; 2.88)**	**Positive**
Land cover area	Built up	0.14	-0.29	0.57	1.15 (0.75 ; 1.77)	-
	Cropland	**-0.23**	**-0.46**	**-0.005**	**0.79 (0.63 ; 0.99)**	**Negative**
	Water	-0.16	-0.44	0.12	0.85 (0.64 ; 1.13)	-
Climatic variables	**Temperature**	**-0.55**	**-0.63**	**-0.48**	**0.57 (0.53 ; 0.62)**	**Negative**
	Precipitation	**0.28**	**0.16**	**0.40**	**1.32 (1.18 ; 1.49)**	**Positive**
	Wind speed	0.12	-0.22	0.46	1.13 (0.80 ; 1.58)	-
Wild animal richness	**Mammal-bird richness**	**1.01**	**0.42**	**1.62**	**2.75 (1.52 ; 5.06)**	**Positive**

Captions

Figure 1: Spatial predictions of all zoonotic emergence risk and associated uncertainty. Panels show (top left) the posterior mean of emergence risk estimated using the INLA model, (top right) the spatial uncertainty expressed as the standard deviation of the latent field, (bottom left) the width of the 95% credible interval, and (bottom right) the resulting hotspot classification combining risk and uncertainty, distinguishing reliable hotspots (high risk and low uncertainty), uncertain hotspots (high risk and high uncertainty), and areas with no detected hotspot.

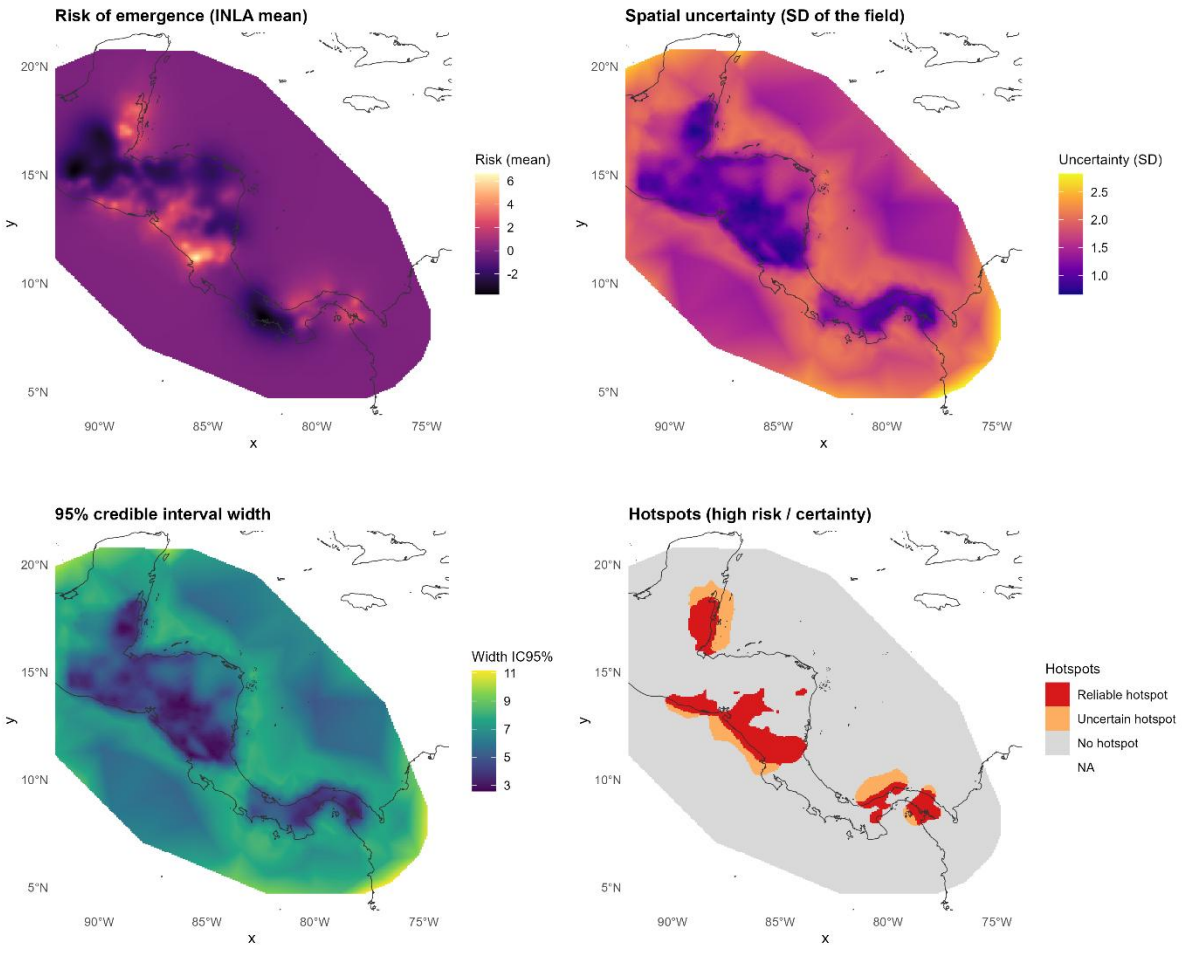

Figure 2: Spatial predictions of *Cochliomyia hominivorax* emergence risk and associated uncertainty. Panels show (top left) the posterior mean of emergence risk estimated using the INLA model, (top right) the spatial uncertainty expressed as the standard deviation of the latent field, (bottom left) the width of the 95% credible interval, and (bottom right) the resulting hotspot classification combining risk and uncertainty, distinguishing reliable hotspots (high risk and low uncertainty), uncertain hotspots (high risk and high uncertainty), and areas with no detected hotspot.

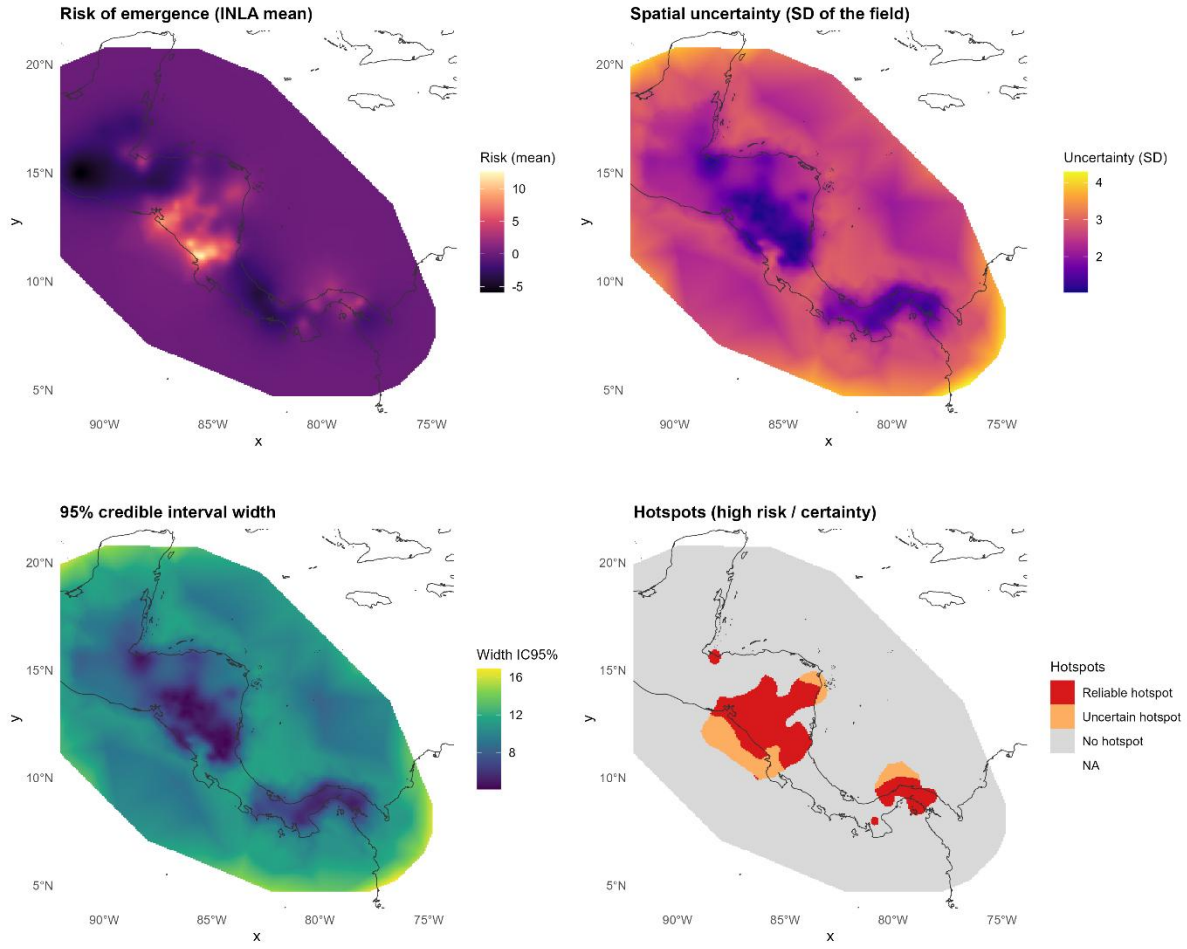

Figure 3: *Nonlinear effect of cattle density on zoonotic occurrence risk.* (A) Posterior smooth effect of cattle density on the probability of zoonotic diseases (all etiologies combined), estimated using a second-order random walk (RW2) model. (B) Corresponding effect estimated only for *Cochliomyia hominivorax* cases. Solid lines represent the posterior mean and shaded regions show the 95% credible intervals.

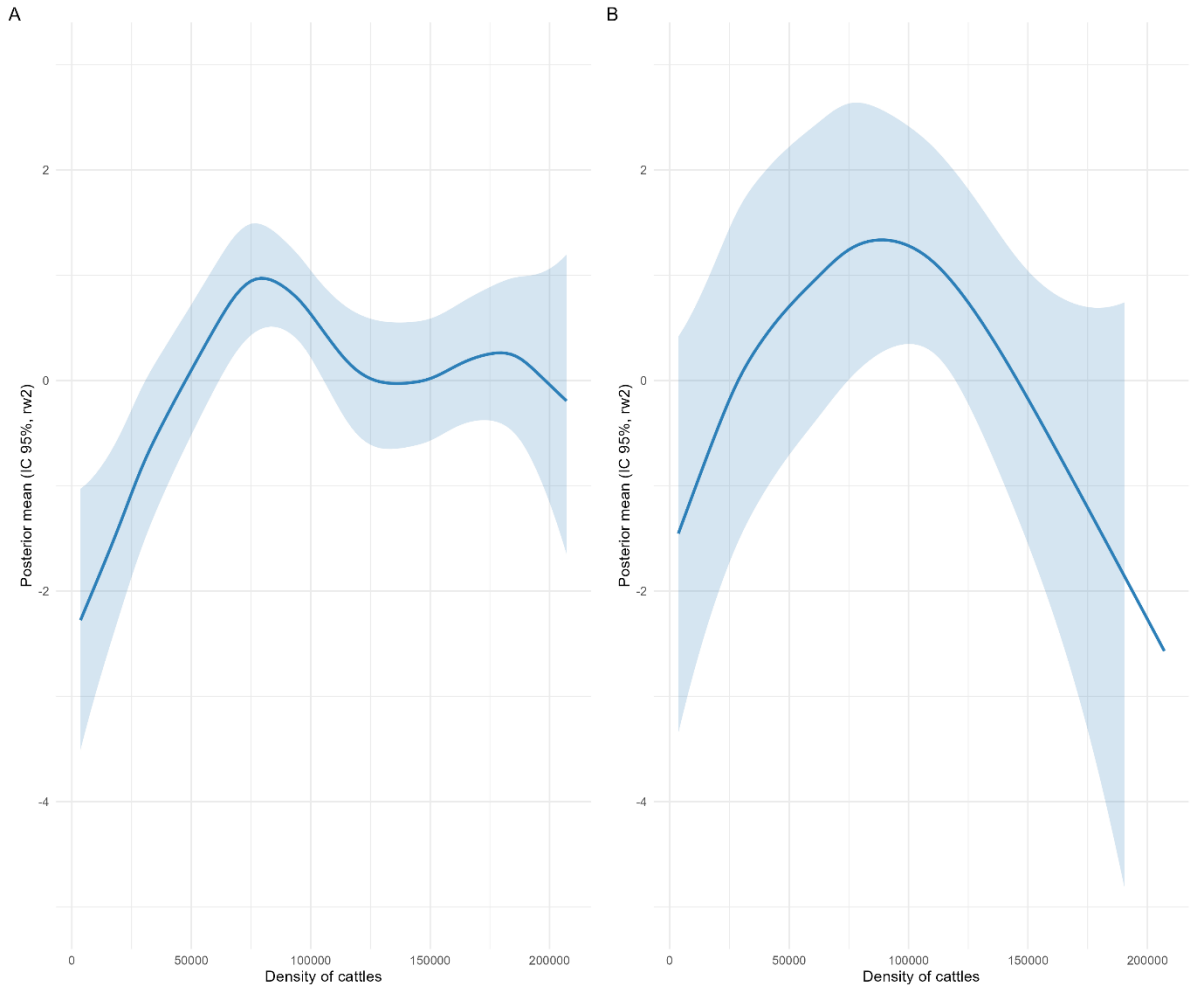

Figure 4. Temporal random effects for zoonotic emergence models (RW1). (A) Posterior temporal random effect for the all-zoonoses emergence model, showing moderate inter-annual fluctuations and a gradual long-term increase across the study period, with a sharp rise beginning around 2020. (B) Posterior temporal random effect for the *Cochliomyia hominivorax*-specific model, characterized by near-zero and highly uncertain effects prior to 2018–2020—reflecting the species' historical near-extinction in Central America—followed by an abrupt and well-supported increase in recent years. Shaded bands represent 95% Bayesian credible intervals (BCIs). Both models were estimated using a first-order random walk (RW1), allowing flexible, data-driven reconstruction of temporal trends.

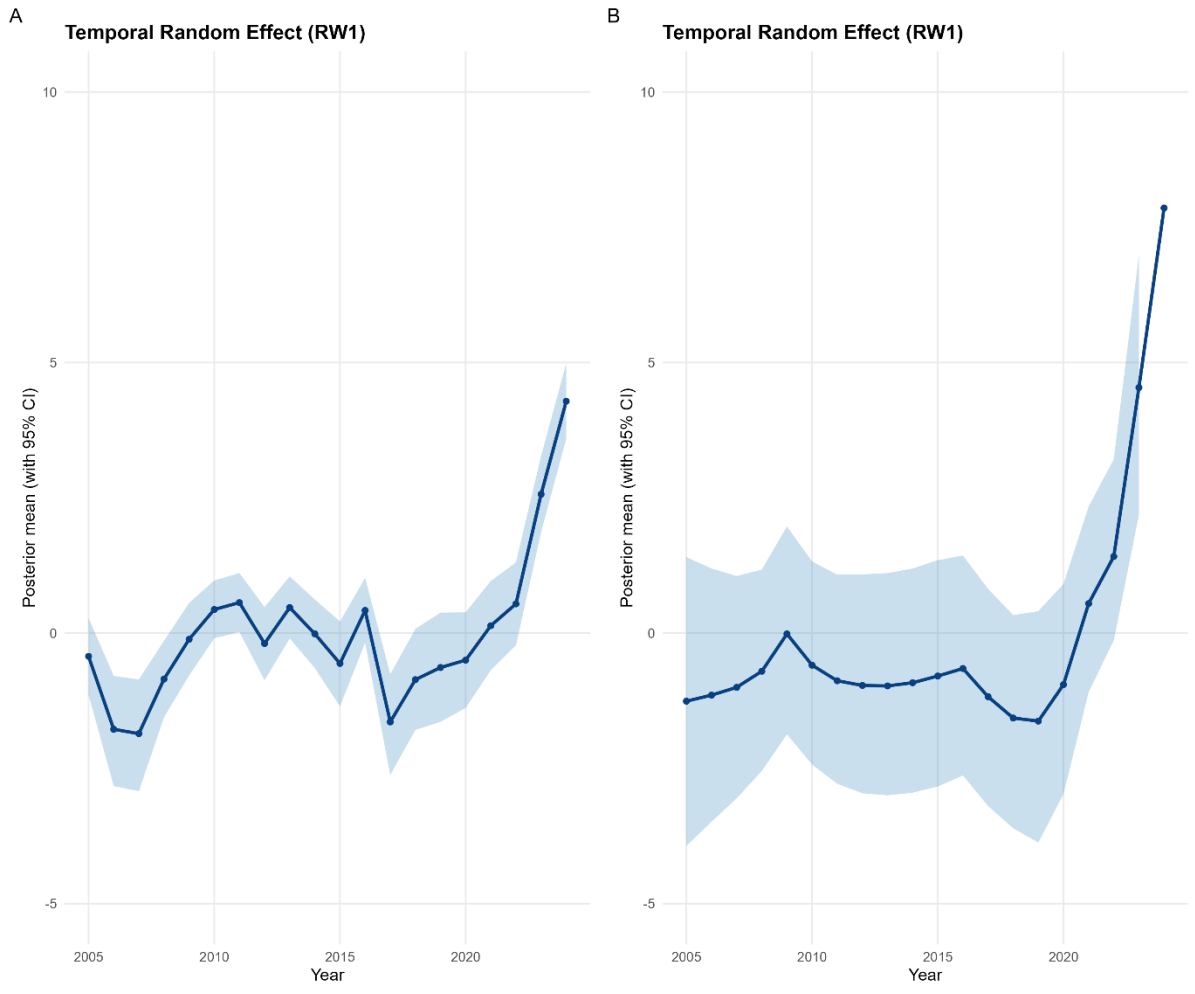

Box 1: From trade-offs to coexistence: A three-dimensional sustainability framework

Reconciling biodiversity conservation with food security is a key sustainability challenge, traditionally framed as a trade-off requiring optimization (Fischer, et al. 2017). Crespin & Simonetti (2021) introduced the concept of *coexistence parameters*, which are the social and ecological factors that can be managed to reduce conflict and shift systems toward states where food security and biodiversity conservation are simultaneously achieved. Such framework conceptualizes the *coexistence niche* as an n-dimensional space located at the intersection of food security and biodiversity components (Crespin et Moreira-Arce 2026).

However, this two-axis model remains incomplete because it lacks a critical third dimension. related to health. As demonstrated by recent global crises, the drivers of biodiversity loss and food insecurity are inextricably linked to zoonotic risk and public health (Hirst et Halsey 2023). Including zoonotic dynamics within the coexistence model thus highlights a key frontier for sustainability science. This manuscript proposes a theoretical expansion of the *Agroecological Systems Model of Coexistence* by formally integrating a third orthogonal axis-health-aligned with the One Health (OH) paradigm (WHO 2022).

Adopting the comprehensive OH definition, the new Health axis is deconstructed into three interdependent components that interact with the original two axes: *Human health*, *Animal health*, and *Environmental health*. Human health encompasses physical health (e.g., free from zoonotic diseases) and mental well-being, the latter often derived from "nature's contributions to people" (NCP) (Díaz, et al. 2018). This component interacts directly with food security access (socioeconomic stability) and biodiversity structure (exposure to green spaces). Animal health integrates the physical health and welfare of both domestic and wild animals, recognizing that high stress in animal populations (driven by habitat fragmentation or intensive agriculture) can compromise immunity and increase pathogen shedding (Hayek 2022). Environmental health refers to the integrity of the physical and biological matrix (e.g., soil, water, air) that acts as the foundational "system context" for human and animal health outcomes. For a complete breakdown of the conceptual components, their specific interactions, and potential parameters within the nexus, see Table 1.

Identifying the points of intersection between these three axes (see Fig.1) allows us to pinpoint the specific coexistence parameters that simultaneously reduce biodiversity impacts, secure food supplies, and mitigate disease risks. For example, managing connectivity through biological corridors is a key coexistence parameter, it restores environmental health and buffers human health risks by regulating vector populations (Ortiz, et al. 2021) (Prist, et al. 2023), while maintaining crop pollination services (food security). Similarly, diversified agroecological systems act as a coexistence parameter by providing stable food while conserving ecological relations that dilute pathogen prevalence among wildlife reservoirs, thus safeguarding animal health (Crespin et Simonetti 2020).

To operationalize this framework, we propose a pragmatic approach grounded in integrated vulnerability mapping. By superimposing data layers for each axis, such as deforestation rates (biodiversity), availability and access indicators (food insecurity) (Sibrian, et al. 2021), and zoonotic risk interfaces (disease burden) (Charles, et al. 2021), we can identify *socio-ecological vulnerability hotspots* where risks converge geographically. This mapping allows us to determine where intervention is most needed to push the local system towards a *basin of coexistence*, a dynamic attractor in phase space where the system remains stable in a state of coexistence despite external shocks (Crespin et Moreira-Arce 2026). By treating human, animal and environmental health as integral components of the coexistence niche, this integration transforms the framework into a comprehensive instrument for regional resilience.

Table 1. Conceptual axes that interact to create the human-nature coexistence nexus. Interactions within the nexus can give way to potential coexistence parameters.

Conceptual Axis	Component	Description	Interactions within the Nexus
Biodiversity	1. Compositional	Identity and variety of genes, species, and populations (e.g., pathogen reservoirs, crop varieties).	→ Food Security: Genetic diversity serves as a buffer for crop resilience (Quantity) and dietary diversity (Quality). → Animal Health: Wild populations act as reservoirs; high diversity can dilute pathogen prevalence (dilution effect). → Human Health: Zoonotic spillover risk increases when compositional balance is disrupted (e.g., loss of predators).
	2. Structural	Physical arrangement of habitats (e.g., forest connectivity, patch size, fragmentation).	→ Environmental Health: Intact structures prevent erosion and regulate microclimates. → Human Health: Fragmentation increases "edge effects," heightening human exposure to vectors like ticks/mosquitoes. → Food Security: Landscape structure determines arable land availability and water retention (Quantity).
	3. Functional	Ecological processes (e.g., nutrient cycling, pollination, predation, water filtration).	→ Food Security: Pollination and soil fertility are critical ecosystem services for crop yields (Quantity). → Environmental Health: Water filtration and air purification directly support the "system context" for health. → Animal Health: Predation regulates reservoir populations, preventing disease outbreaks.
Food Security	1. Quantity (Availability)	The supply of food (calories) dependent on production systems and land use.	→ Biodiversity: Expansion of production often degrades Structural biodiversity (deforestation). → Animal Health: Intensification (crowding) increases stress and pathogen transmission in livestock. → Environmental Health: Agrochemical use can degrade soil and water quality.
	2. Quality (Utilization)	Nutritional value, food safety, and diet diversity required for healthy metabolism.	→ Human Health: Adequate nutrition supports immune function (Physical); nutritional deficiencies increase vulnerability to disease. → Biodiversity: Demand for diverse diets encourages the conservation of agrobiodiversity (Compositional) rather than monocultures.
	3. Access & Stability	Physical/economic access to food and the stability of that access over time.	→ Human Health: Poverty and food insecurity drive stress (Mental Health) and reliance on unsafe foods. → Biodiversity: Instability drives coping strategies like bushmeat hunting, impacting wildlife populations (Compositional). → Animal Health: Unregulated trade or hunting compromises wildlife welfare and health.

Health	1. Human Health	Physical: Freedom from disease/injury. Mental: Well-being and resilience.	→ Biodiversity: "Nature's contributions to people" (NCP) support mental well-being (Structural). → Food Security: Healthy populations are economically productive, ensuring stable food access (Access).
	2. Animal Health	Physical: Disease status of domestic/wild animals. Welfare: Freedom from distress (Five Freedoms).	→ Biodiversity: Disease outbreaks in wildlife (e.g., chytrid, distemper) can cause extinction events (Compositional). → Food Security: Healthy livestock ensures stable protein supplies; sick animals threaten food safety (Quality).
	3. Environmental / Ecosystem Health	Integrity of the physical environment (soil, water, air) that sustains life.	→ Biodiversity: A healthy matrix supports functional ecosystem processes (Functional). → Food Security: Degraded environments (e.g., salinized soil) collapse production systems (Quantity).

Box 2. Glossary of concepts for the expanded Coexistence Nexus Framework. The following terms are fundamental to the expanded conceptual model presented in Box 1 and detailed in Table 1.

Term	*Definition*
Agroecological Systems Model of Coexistence	The original conceptual framework that established the Food-Biodiversity nexus, composed of two multidimensional axes (Food Security and Biodiversity), which this manuscript expands upon (Crespin & Simonetti 2021).
Coexistence Niche	A multi-dimensional subspace where both food production and biodiversity conservation needs are met. It is an n-dimensional space located at the intersection of various components of food security and biodiversity (Crespin & Moreira-Arce 2026).
Coexistence Parameters	Social and ecological factors that can be actively managed to reduce conflict and shift a social-ecological system toward a state where food security and biodiversity are simultaneously achieved (Crespin & Simonetti 2021).
Coexistence Nexus	The expanded conceptual framework resulting from formally integrating the third orthogonal axis of Health (One Health) into the original Food-Biodiversity nexus (Crespin & Moreira-Arce 2026).
One Health (OH)	A comprehensive approach recognizing that the health of humans is inextricably linked to the health of animals and the environment (One Health High-Level Expert Panel et al. 2022).
Human Health	A component of the Health axis encompassing both physical health (e.g., freedom from zoonotic diseases) and mental well-being, the latter often derived from "nature's contributions to people" (NCP) (Díaz et al. 2018).
Animal Health	A component of the Health axis that integrates the physical health and welfare of both domestic and wild animals, including their disease status and freedom from distress and fear (One Health High-Level Expert Panel et al. 2022).
Environmental/Ecosystem Health	A component of the Health axis referring to the integrity of the physical and biological matrix (e.g., clean water, soil stability) that acts as the foundational "system context" for all other health outcomes (One Health High-Level Expert Panel et al. 2022).
Socio-ecological vulnerability hotspots	Specific geographic locations identified by integrated vulnerability mapping where critical risks from biodiversity erosion, food insecurity, and disease burden converge, requiring targeted intervention.
Basin of Coexistence	Not a physical place, but a dynamic attractor in phase space where a social-ecological system remains stable in a desired state of coexistence despite external shocks or perturbations (Crespin & Moreira-Arce 2026).